Universal Berezinskii-Kosterlitz-Thouless dynamic scaling in the intermediate timerange in frustrated Heisenberg antiferromagnets on triangular lattice

Ivan S. Popov, Pavel V. Prudnikov
Omsk State University, pr. Mira 55, Omsk 644077 Russia

Andrey N. Ignatenko
Institute of Metal Physics, 620990, Kovalevskaya str. 18 Ekaterinburg, Russia

Andrey A. Katanin
Institute of Metal Physics, 620990, Kovalevskaya str. 18 Ekaterinburg, Russia and
Ural Federal University, 620002, Mira str. 19, Ekaterinburg, Russia

arXiv:1611.04710v1 [cond-mat.str-el] 15 Nov 2016

We investigate non-equilibrium properties of the frustrated Heisenberg antiferromagnets on the triangular lattice. Nonequilibrium critical relaxation of frustrated Heisenberg antiferromagnets shows a sharp dynamic topological Berezinskii-Kosterlitz-Thouless transition at the same temperature $T_{\rm BKT} = 0.282J$ as for static properties, due to the pairing of vortices at $T < T_{\rm BKT}$. We show that starting from the high-temperature initial state in a broad temperature range $T < T_{\rm BKT}$ the dynamic properties at the intermediate time range are similar to those of two-dimensional XY model due to presence of $\mathbb{Z}_2$-vortices in the considering system. The interaction of vortices with spin-wave degrees of freedom does not emerge until rather long times.

PACS numbers: 68.35.Rh, 64.60.De, 64.60.Ht, 75.40.Mg

Investigations of critical behavior in systems with continuous symmetry of the order parameter attract a lot of attention and represent considerable fundamental and practical interest [1]. Strong fluctuation effects playing an important role in low dimensional [2, 3] and frustrated [4] systems, may lead to non-trivial critical behavior of these systems.

In two-dimensional systems with continuous symmetry of the order parameter the long-range order at finite temperatures is destroyed by spin fluctuations [5]. Presence of topologically non-trivial configurations (vortices), however, leads to the peculiarities of the disordered (paramagnetic) state. In particular, a topological phase transition, associated with the dissociation of vortex pairs, occurs at a temperature $T_{\rm BKT} \neq 0$, as was shown by Berezinskii [6, 7], and then Kosterlitz and Thouless [8, 9]. Below $T_{\rm BKT}$ vortices are bound in pairs, the correlation length is infinite, and there is an algebraic (power-law) decay of spin correlators. This changes at $T > T_{\rm BKT}$, when vortices are not bound, causing finite correlation length. The presence of vortices in non-equilibrium states (even below $T_{\rm BKT}$) may change essentially the dynamical properties of the system. In particular, in Ref. [10] it was shown that in the presence of vortices the time dependence of the correlation length $\xi(t) = (t/\ln t)^{1/2}$ acquires logarithmic correction.

Magnetic frustration, which occurs due to peculiarities of lattice geometry, yields on one hand an enhancement of the fluctuation effects, but on the other hand, provides a possibility of realizing new types of topological structures with respect to those in non-frustrated systems. Experimental studies of magnetic materials with triangular lattice, in particular $NaCrO_2$ [11–14], $NiGa_2S_4$ [15–21], $\kappa-(BEDT-TTF)_2Cu_2(CN)_3$ [22–24] $EtMe_3Sb[Pd(dmit)_2]_2$ [25, 26], reveal distinct anomaly behavior at non-zero temperatures, typical of phase transitions and non-trivial dynamic properties above and below the observed phase transition [11, 14, 17, 19, 20].

Equilibrium properties of frustrated antiferromagnets on a triangular lattice exhibit features of the Berezinskii-Kosterlitz-Thouless phase transition similar to 2D XY-model [27, 28] This is associated with the presence of $\mathbb{Z}_2$-vortices, which are also bounded to vortex pairs at temperatures below a certain characteristic temperature $T_{\rm BKT}$, which allows to draw an analogy between the low temperature properties of this system and critical properties of 2D XY model. In contrast to the XY model, for frustrated magnetic materials the correlation length is finite even below $T_{\rm BKT}$ due to the contribution of non-topological (or spin-wave) degrees of freedom [29–33].

The finiteness of the correlation lenght leads to the question, to what extent the dynamic properties of frustrated systems are similar (or different) to those of the XY-model, in particular whether peculiar phenomena of the nonequilibrium critical dynamics, such as dynamic scaling and aging effects [34–38], occur in the low-temperature phase $T < T_{\rm BKT}$. In the present paper we show, that at intermediate timescales the dynamic properties of frustrated magnets are in fact very similar to those of XY model. At very long timescales the dynamic properties change due to the finiteness of the equilibrium correlation lenght, but the latter scale is extremely large even for not too low temperatures.

Below we consider the non-equilibrium dynamics of the frustrated Heisenberg model on a triangular lattice

$$H = J \sum_{<i,j>} \mathbf{S}_i \mathbf{S}_j, \qquad (1)$$

where $J > 0$ is the exchange integral, which is taken as a unit of energy in the present study, $\mathbf{S}_i$ are classical Heisenberg spins located at sites i of the two-dimensional triangular lattice, $< i, j >$ denotes summation over the nearest neighbors of the lattice. The ground state of the system has the form of 120-degree order with the wave vector $\mathbf{Q} = (4\pi/3, 0)$.

For a numerical study of the nonequilibrium relaxation, we perform Monte-Carlo simulations using Metropolis algorithm [39]. Although equilibrium properties were intensively studied previously [27, 31–33, 40–43], the investigation of the non-equilibrium processes allows us to get information on the dynamic properties of the frustrated systems. Time is set in Monte Carlo steps per spin MCS/s, which defines the time interval during which each of $N = L^2$ spins have the ability to change its state. We consider lattices with sizes $L \leq 240$.

The low-temperature ordered state corresponds to the ground state of the system with the initial temperature $T_L^{\rm ini} = 0$. This initial state does not have vortex excitations. In contrast to this initial state, the high temperature initial state is prepared at temperature $T_H^{\rm ini} = 20 \gg T_{\rm BKT}$ where the concentration of free vortices is much larger than at the equilibrium.

Starting from the low-temperature initial state, which is characterized by an infinitely large correlation length, the correlation length in the process of relaxation drops to its equilibrium value determined by the temperature and the linear size of the system (see Fig. 1a). One can see the existence of a certain characteristic Berezinskii-Kosterlitz-Thouless temperature $T_{\rm BKT} \approx 0.3$, at which the correlation length at short time scales drops substantially, yielding also shorter correlation length in the limit of long times.

The temperature $T_{\rm BKT}$ in equilibrium can be accurately determined from the temperature dependence of the equilibrium order parameter $S(T) = \sqrt{|\mathbf{S_Q}|^2}$, where $\mathbf{S_Q} = (1/N)\sum_i e^{i\mathbf{Q}\mathbf{R}_i}\mathbf{S}_i$, which decreases with temperature, dropping at some (size-dependent) characteristic temperature $T^*(L)$ (see Fig. 1b). The dependence of the position of the inflection points $T^*(L)$ of the temperature dependence of the order parameters determines $T_{\rm BKT}$ and (quasi) critical exponent of the temperature dependence of correlation length of vortex subsystem $\xi_v \propto \exp(A/(T - T_{\rm BKT})^\nu)$ according to

$$T^*(L) = T_{\rm BKT} + A/(\ln L)^{1/\nu}. \qquad (2)$$

From fitting the least squares, we find $T_{\rm BKT} = 0.2820(5)$ and $\nu = 0.37(1)$. The temperature $T_{\rm BKT}$ agrees well and the index ν agrees qualitatively with previous results $T_{\rm BKT} = 0.285(5)$, $\nu = 0.42 \pm 0.15$ of Ref. [33].

In contrast to the XY model, the equilibrium correlation length at $T < T_{\rm BKT}$ is finite, although exponentially large at low temperatures $T \ll J$, where it is determined by long wavelength spin-wave fluctuations [29],

$$\xi_{\rm sw}(T) \propto a \exp \frac{\pi(2+\pi)\rho_\perp}{2T}, \qquad (3)$$

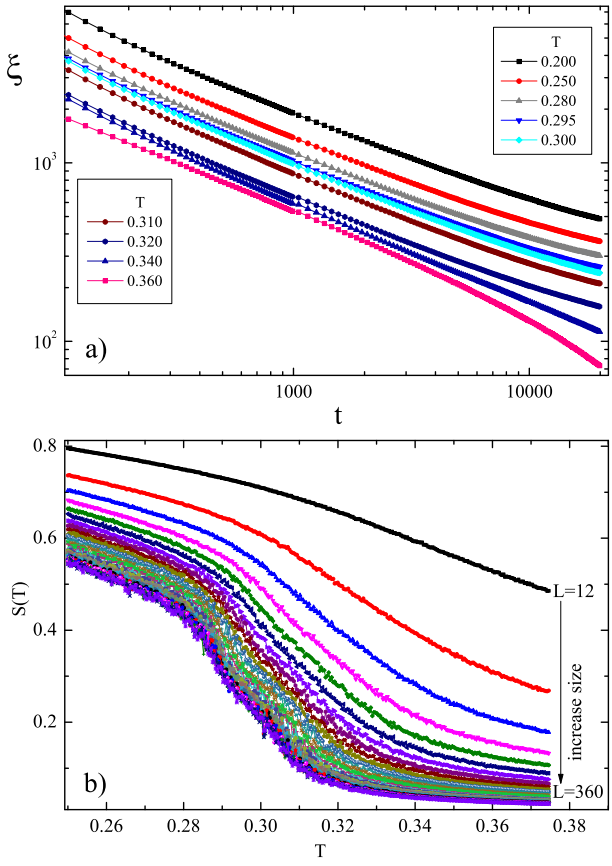

FIG. 1. (Color online) (a) The time dependence of the correlation length of the system at nonequilibrium evolution from the low-temperature initial state for the linear size $L = 240$. (b) The temperature dependence of the equilibrium order parameter $S(T)$ for various sizes of the system L.

($\rho_\perp$ denotes transverse spin stiffness [39]). As we argue below, the correlation length (3) provides an additional length scale not only for the equilibrium but also for the dynamics. In the considered system the equilibrium spin-wave fluctuations interact with vortices and wash out completely the specific spin configuration of vortex at distances $r \gg \xi_{\rm sw}$ from the vortex core. As a result, two vortices almost cease to interact at distances $r \gg \xi_{\rm sw}$.

In case of relaxation of the nonequilibrium high-temperature disordered initial state to the low-temperature equilibrium, the initial state contains many free vortices that are attracted to each other and annihilate as relaxation proceeds (see Fig. 2). Against the background of this slow movement there is also more rapid spin wave dynamics, which is not related to a change in positions of vortex cores. Because of difference of characteristic times of the vortices and spin waves, the coarse-grained description of the relaxation process on basis of the adiabatic approximation becomes possible. Assuming that the spin-wave subsystem is already in the local (intermediate) thermodynamic equilibrium for each current position of the vortex cores, the relaxation of the

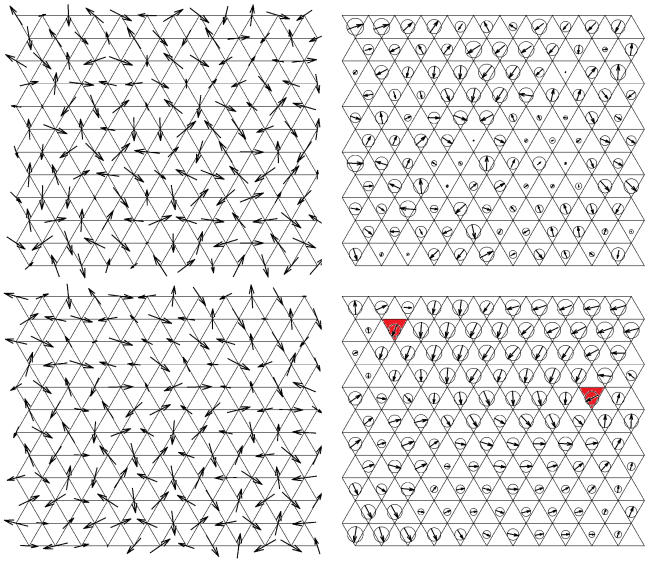

FIG. 2. (Color online) Snapshot of relaxation dynamics of system at $T = 0.1$ and the times 100 (upper plots) and 15000 (lower plots) MCS/s from the high temperature initial state. Left (right) figures – projections of the spins (chiriality) vectors onto the xy-plane. The radius of a circle on left figures represents the length of each chiriality vector. Red triangles on right lower figure denote cores of $\mathbb{Z}_2$-vortices; the vortices on the upper figure are not shown: because of their large number, it is impossible to identify them uniquely.

correlation length for the high temperature initial state is described by the equation (see Supplementary Material [39])

$$\frac{d\xi^2}{dt} = \frac{4\Gamma \ln(\xi_{\rm sw}/\xi)}{\ln(\xi/a)\left[2\ln(\xi_{sw}/\xi) + \ln(\xi/a)\right]}, \quad a \ll \xi. \qquad (4)$$

where Γ is the kinetic coefficient, a is the lattice parameter. At not too long times $t \ll \xi_{\rm sw}^2/8\Gamma$ we obtain the same $(t/\ln t)^{1/2}$ time dependence, as in the XY model.

On Fig. 3 we present the time dependence of the correlation length of the system from the initial high-temperature state, obtined from the Monte-Carlo calculation, and plot as a function of $t/\ln t$ in a logarithmic scale. The obtained time dependence confirms the above result, reflecting violation of dynamic scaling and influence on the dynamics of vortex pairs, which are present in the system. We observe that at low temperatures $T \leq 0.2$, and short time scale $\leq 100 - 1000$ MCS/s there is a deviation from the universal dependence. The time of the onset of scaling behavior increases with decreasing temperature and agrees with the time of the onset of strong short-range order $t_{\rm SRO}$ (see Supplementary Material [39]). Therefore, the observed deviation from scaling behavior corresponds to the not fully formed short range magnetic order (see upper part of Fig. 2 for typical spin configuration), when vortices and spin waves are not yet well-defined.

Let us now turn to the time dependence of the auto-

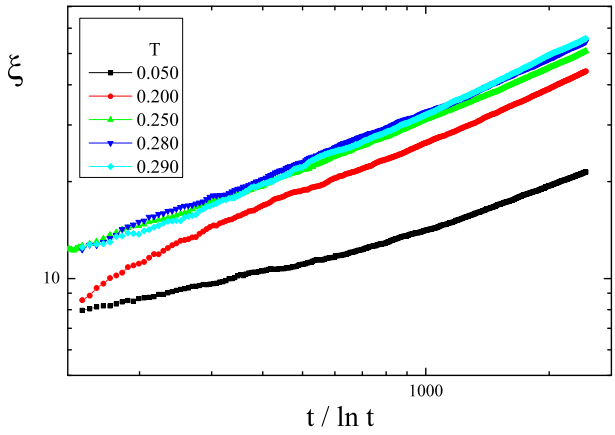

FIG. 3. (Color online) The time dependence of the correlation length of the system at nonequilibrium evolution from the high-temperature initial state for the linear size $L = 240$.

correlation function

$$C(t, t_w) = \frac{1}{N}\sum_i \langle \mathbf{S}_i(t)\mathbf{S}_i(t_w)\rangle\,. \qquad (5)$$

We have observed presence of the aging effects (slowing of the relaxation processes by increasing the waiting time t_w) in the system for temperatures $T < 0.35$ (for higher temperatures obtained dependences can not be attributed to the aging effects, they rather show non-uniform in time nonequilibrium relaxation). With the start from the initial high-temperature state we find slowdown in the time decay of the autocorrelation function with increasing waiting time t_w, while with the start from the initial low-temperature state the observed effects are opposite, and autocorrelation function decay is accelerated with increasing waiting time t_w.

The important feature of the aging is the scaling behavior, which is obeyed by autocorrelation function in accordance with the general considerations of critical dynamics [44, 45],

$$C(t, t_w) = (t - t_w)^{\eta/2}\Phi(\xi(t - t_w)/\xi(t_w)), \qquad (6)$$

where η is the anomalous dimension, depending on the temperature. On Fig. 4a-c we present obtained scaling laws for two-time dependencies of the autocorrelation function according to the Eq. (6). One can see that in the low temperature phase the scaling of the autocorrelation function is fulfilled, but it begins to break after passing to the high-temperature phase $T > T_{\rm BKT}$. On Fig. 4d we present the extracted temperature dependence of the critical exponent η. One can see, that at the Berezinskii-Kosterlitz-Thouless temperature $T_{\rm BKT}$ the critical exponent is close to the value $\eta(T_{\rm BKT}) = 0.25$ for the XY-model.

Thus from the above consideration we conclude that on the intermediate time range the scaling properties of the frustarted Heisenberg model on the triangular lattice are the same (or, at least very close) to those for

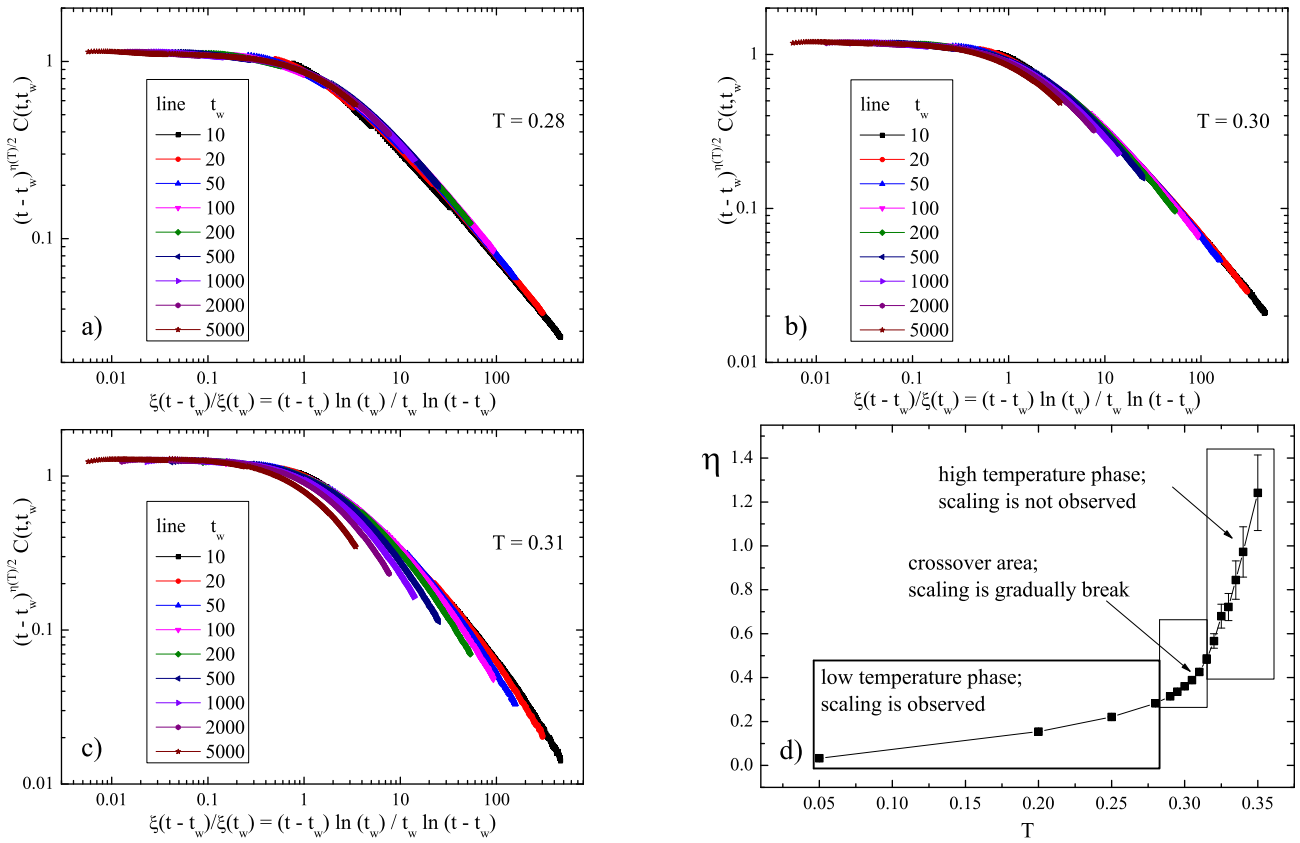

FIG. 4. (Color online) (a-c) Scaling for the autocorrelation function of the system with $L = 240$; $T = 0.28$, 0.3, and 0.31 from the high-temperature initial state. (d) The temperature dependence of the anomalous dimension $\eta(T)$.

the XY model: we observe $(t/\ln t)^{1/2}$ time dependence of the correlation length and fufillment of the scaling law (6) in a broad time range at $T \leq T_{\rm BKT}$, despite finite value of the correlation length in this temperature range. This reflects the absence of unbound vortices in the low-temperature phase $T < T_{\rm BKT}$ in a two-dimensional frustrated antiferromagnetic Heisenberg model (or, at least, their vanishingly small concentration), and surprisingly weak effects of interaction between vortices and spin-wave degrees of freedom.

These results demonstrate significant difference in the dynamics of the system above and below $T_{\rm BKT}$, such that the obtained temperature $T_{\rm BKT}$ can be considered as the temperature of the dynamic transition (or, at least, sharp crossover), related to the vortex unbinding.

In conclusion, we have calculated time dependence of the correlation length and spin correlation functions for Heisenberg antiferromagnet on the triangular lattice and have shown, that in the intermediate timerange they fulfill scaling relations, identical to those, which were found earlier for the XY model. Therefore, the dynamic properties of the triangular lattice antiferromagnets in this timerange originate mainly from the $\mathbb{Z}_2$-vortices, which contribute the dynamics similarly to the vortices of the XY model. At very short times we have observed some deviations from the scaling laws, which originate from the absence of well defined spin-wave and vortex excitations in the lack of short-range magnetic order. At very long times the contribution of the (equilibrated) spin waves, which provide finite correlation length below Berezinskii-Kosterlitz-Thouless transition, becomes important.

Acknowledgements. The work was performed within the grant No. MD-6024.2016.2 of Russian Federation President (I.P., P.P.), themes "Quant" 01201463332 (A. I.) and "Electron" 01201463326 (A. K.) of FASO, Russian Federation, and partially supported within the projects of Russian Foundation of Basic Research 14-32-50632-mol-nr (I.P.) and 14-02-00953a (A.I., A.K., I.P.). The calculations are performed on the Supercomputing Center of Lomonosov Moscow State University, Moscow Joint Supercomputer Center and St. Petersburg Supercomputer Center of the Russian Academy of Sciences.

[1] S.-K. Ma, *Modern theory of critical phenomena*, Westview Press (New York, 2000).

[2] A. Auerbach, *Interacting electrons and quantum mag-*

netism, Spriner (New York, Berlin, 1994).
[3] L. G. De Jongh (ed.), *Magnetic Properties of Layered Transition Metal Compounds*, Kluwer Academic Publishers (Dordrecht, Boston, London, 1990).
[4] C. Lacroix, P. Mendels, and F. Mila (eds.), *Introduction to frustrated magnetism*, Springer-Verlag (Berlin, Heidelberg, 2011).
[5] N.D. Mermin, H. Wagner, Phys. Rev. Lett. **17** 1133 (1966).
[6] V. L. Berezinskii, Sov. Phys. JETP **32**, 493 (1971); **34**, 610 (1972).
[7] V. L. Berezinskii, *Low-Temperature Properties of Two-Dimensional Systems* (Fizmatlit, Moscow, 2007) [in Russian].
[8] J.M. Kosterlitz, D.J. Thouless, J.Phys.C. **6** 1181 (1973).
[9] J.M. Kosterlitz, J. Phys. C. **7** 1046 (1974).
[10] A. J. Bray, A. J. Briant, and D. K. Jervis. Phys. Rev. Lett. **84**, 1503 (2000).
[11] A. Olariu, P. Mendels, F. Bert, B. G. Ueland, P. Schiffer, R. F. Berger, R. J. Cava, Phys. Rev. Lett. **97**, 167203 (2006).
[12] D. Hsieh, D. Qian, R. F. Berger, R. J. Cava, J. W. Lynn, Q. Huang, M. Z. Hasan, Physica B **403**, 1341 (2008).
[13] D. Hsieh, D. Qian, R. F. Berger, R. J. Cava, J. W. Lynn, Q. Huang, M. Z. Hasan, J. Phys. Chem. Solids **69**, 3174 (2008).
[14] M. Hemmida, H.-A. Krug von Nidda, N. Buttgen, A. Loidl, L. K. Alexander, R. Nath, A. V. Mahajan, R. F. Berger, R. J. Cava, Y. Singh, D. C. Johnston, Phys. Rev. B **80**, 054406 (2009).
[15] S. Nakatsuji, Y. Nambu, H. Tonomura, O. Sakai, S. Jonas, C. Broholm, H. Tsunetsugu, Y. Qiu, Y. Maeno, Science **309**, 1697 (2005).
[16] Y. Nambu, S. Nakatsuji, Y. Maeno, J. Phys. Soc. Jpn. **75**, 043711 (2006).
[17] H. Takeya, K. Ishida, K. Kitagawa, Y. Ihara, K. Onuma, Y. Maeno, Y. Nambu, S. Nakatsuji, D. E. MacLaughlin, A. Koda, R. Kadono, Phys. Rev. B **77**, 054429 (2008).
[18] A. Yaouanc, P. D. de Reotier, Y. Chapuis, C. Marin, G. Lapertot, A. Cervellino, A. Amato, Phys. Rev. B **77**, 092403 (2008).
[19] D. E. MacLaughlin, Y. Nambu, S. Nakatsuji, R. H. Heffner, L. Shu, O. O. Bernal, K. Ishida, Phys. Rev. B **78**, 220403(R) (2008).
[20] H. Yamaguchi, S. Kimura, M. Hagiwara, Y. Nambu, S. Nakatsuji, Y. Maeno, K. Kindo, Phys. Rev. B **78**, 180404 (2008).
[21] H. Yamaguchi, S. Kimura, M. Hagiwara, Y. Nambu, S. Nakatsuji, Y. Maeno, A. Matsuo, K. Kindo, J. Phys. Soc. Jpn. **79**, 054710 (2010).
[22] Y. Shimizu, K. Miyagawa, K. Kanoda, M. Maesato, G. Saito, Phys. Rev. Lett. **91**, 107001 (2003).
[23] S. Yamashita, Y. Nakazawa, M. Oguni, Y. Oshima, H. Nojiri, Y. Shimizu, K. Miyagawa, K. Kanoda, Nat. Phys. **4**, 459 (2008).
[24] M. Yamashita, N. Nakata, Y. Kasahara, T. Sasaki, N. Yoneyama, N. Kobayashi, S. Fujimoto, T. Shibauchi, Y. Matsuda, Nat. Phys. **5**, 44 (2009).
[25] M. Tamura, A. Nakao, R. Kato, J. Phys. Soc. Jpn. **75**, 093701 (2006).
[26] T. Itou, A. Oyamada, S. Maegawa, M. Tamura, R. Kato, Phys. Rev. B **77**, 104413 (2008).
[27] H. Kawamura, S. Miyashita, J. Phys. Soc. Jpn. **53**, 4138 (1984).
[28] H. Kawamura, J. Phys.: Conf. Ser. **320**, 012002 (2011).
[29] P. Azaria, B. Delamotte, and D. Mouhanna. Phys. Rev. Lett., **68**, 1762 (1992).
[30] A. N. Ignatenko, V. Yu. Irkhin, and A. A. Katanin, Nucl. Phys. B **814**, 439 (2009).
[31] B. W. Southern, A. P. Young, Phys. Rev. B **48**, 13170 (1993).
[32] M. Wintel, H.U. Everts, W. Apel, Phys. Rev. B **52**, 13480 (1995).
[33] H. Kawamura, A. Yamamoto, T. Okubo, J. Phys. Soc. Jpn. **79**, 023701 (2010).
[34] P. V. Prudnikov, V. V. Prudnikov, and I. S. Popov, JETP Letters **101**, 539 (2015).
[35] L. Berthier, J. Kurchan, Nature Phys. **9**, 310 (2013).
[36] S. Ciliberto, R. Gomez-Solano, A. Petrosyan, Annu. Rev. Condens. Matter Phys. **4**, 11 (2013).
[37] L. Berthier, P.C.W. Holdsworth, M. Sellitto J. Phys. A **34**, 1805 (2001).
[38] S. Abriet, D. Karevski, Eur. Phys. J. B **37**, 47 (2004).
[39] See Supplementary Material on the details of the Metropolis algorithm, time- and temperature dependence of the short-range order parameters, and dynamics of correlation length in the presence of vortices.
[40] H. Kawamura, M. Kikuchi, Phys. Rev. B **47**, 1134 (1993).
[41] B. W. Southern, H-J. Xu, Phys. Rev. B **52**, R3836 (1995).
[42] M. Caffarel, P. Azaria, B. Delamotte, and D. Mouhanna, Phys. Rev. B **64**, 014412 (2001).
[43] H. Kawamura, A. Yamamoto, J. Phys. Soc. Jpn. **76**, 073704 (2007).
[44] M. Henkel, M. Pleimling, Non-Equilibrium Phase Transitions, Vol. 2, Heidelberg: Springer. 2010.
[45] M. Henkel et al. Ageing and the Glass Transitions. Heidelberg: Springer. 2007.

SUPPLEMENTARY MATERIAL TO THE PAPER

Universal Berezinskii-Kosterlitz-Thouless dynamic scaling in the intermediate timerange in frustrated Heisenberg antiferromagnets on the triangular lattice

I. S. Popov, P. V. Prudnikov, A. N. Ignatenko, and A. A. Katanin

A. Metropolis algorithm

The sequence of states defined by the Metropolis algorithm according to the transition probability between neighboring configurations, forms a Markov process. The evolution of the nonequilibrium distribution function $P_n(t)$ can be written in the form of the master kinetic equation:

$$\frac{dP_n(t)}{dt} = \sum_m W(n \to m)P_n(t) - \sum_m W(m \to n)P_m(t), \tag{S1}$$

where $W(n \to m) = \min\left[1.0, \exp(-\Delta E_{nm}/T)\right]$. Initial low- and high temperature states are visualized in Fig. S1.

The time dependence of correlation length $\xi(t)$ can be defined as follows:

$$\xi(t) = \frac{3L}{4\pi}\sqrt{\frac{\chi(t)}{\Phi(t)} - 1}, \tag{S2}$$

where

$$\chi(t) = \left\langle \left|\mathbf{S}_Q(t)\right|^2 \right\rangle - \left\langle \left|\mathbf{S}_Q(t)\right| \right\rangle^2 \tag{S3}$$

is the susceptibility, and

$$\Phi(t) = \frac{1}{2}\sum_{n=x,y}\left\langle \left| \sum_i \mathbf{S}_i(t) e^{i\mathbf{q}_n\mathbf{R}_i + i\mathbf{Q}\mathbf{R}_i} \right|^2 \right\rangle \tag{S4}$$

is the structural factor of system.

To analyze the dynamic behavior of magnetic order, in addition to $\chi(t)$ we have investigated the time dependence of the short-range order parameter $K(t)$

$$K(t) = \frac{1}{2N}\left\langle \sum_{\mathbf{r}} \left|\mathbf{k}(\mathbf{r},t)\right| \right\rangle, \tag{S5}$$

determined by local field of vector chirality $\mathbf{k}(\mathbf{r},t)$

$$\mathbf{k}(\mathbf{r},t) = \frac{2}{3\sqrt{3}}\left(\mathbf{S}_1 \times \mathbf{S}_2 + \mathbf{S}_2 \times \mathbf{S}_3 + \mathbf{S}_3 \times \mathbf{S}_1\right), \tag{S6}$$

where the summation is meant for all the elementary triangles of the lattice and spins with numbering 1, 2 3 correspond to anti-clockwise circumvent of triangles. Snapshots of spin configurations at different times are presented in Fig. 2 of the main text and Fig. S2 of this material.

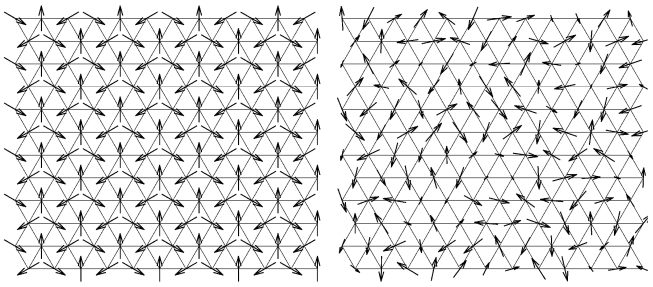

FIG. S1. Projection of spin vectors onto xy plane for the initial low- and high temperature states of MC simulation

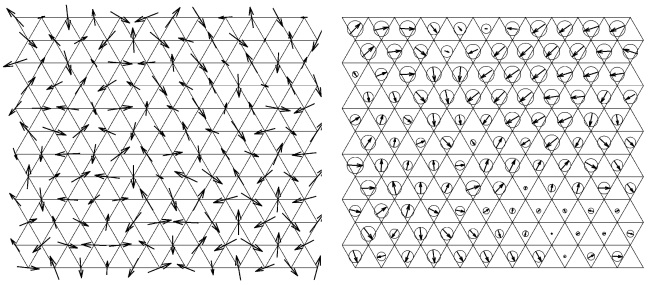

FIG. S2. Snapshot of relaxation dynamics of system at $T = 0.1$ and the times 5000 MCS/s from the high temperature initial state. Left (right) figures – projections of the spins (chiriality) vectors onto the xy-plane.

The temperature dependence of the equilibrium order parameter is shown in Fig. 1b of the main text. These data are used to extract the value of the Berezinskii-Kosterlitz-Thouless temperature T_{BKT} and the exponent ν according to the equation (2) of the main text.

Fig. S3 shows the obtained time dependence $K(t)$ at various temperatures and temperature dependence of the equilibrium short-range order parameter of the system $K_T = K(t \to \infty)$. One can observe that the characteristic time of the onset of the equilibrium short-range order parameter t_{SRO} increases with decreasing temperature, and agrees with the time scale, starting from which the scaling of the time dependence of correlation length is observed, starting from the high-temperature initial state (see Fig. 3 of the main text). The equilibrium short-range order parameter K_T monotonously decreases with temperature, and does not have any peculiarity (except possible inflection point) near $T_{\mathrm{BKT}} = 0.282$.

B. Dynamics of $\mathbb{Z}_2$-vortices in the triangular lattice antiferromagnet

The dynamics of the triangular lattice Heisenberg antiferromagnet can be described by fluctuating order parameter having the form of continuous vector fields $\mathbf{e}_1(\mathbf{x})$,

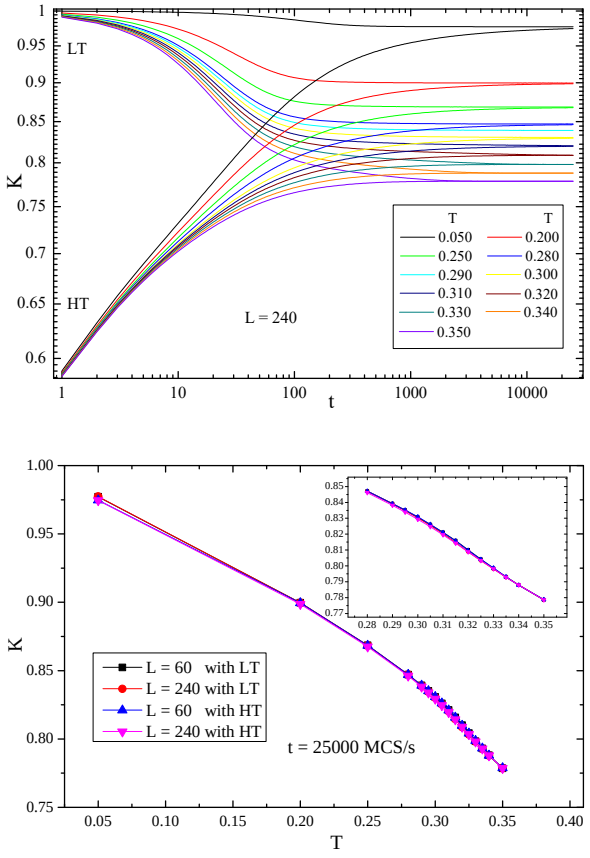

FIG. S3. Upper plot: the time dependence of the short range order parameter starting from the low-temperature (LT) and high-temperature (HT) initial state at L=240. Lower plot: temperature dependence of the equilibrium short-range order parameter for various L. The inset shows the behavior in the vicinity of Berezinskii-Kosterlitz-Thouless temperature.

$\mathbf{e}_2(\mathbf{x})$ defined by the equation

$$\mathbf{S}_i = \mathbf{e}_1(\mathbf{R}_i)\cos(\mathbf{Q}\cdot\mathbf{R}_i) + \mathbf{e}_2(\mathbf{R}_i)\sin(\mathbf{Q}\cdot\mathbf{R}_i). \qquad \text{(S7)}$$

These fields evolve in time according to a stochastic equation

$$\frac{\partial \mathbf{e}_\alpha(\mathbf{x},t)}{\partial t} = -\Gamma\frac{\delta H}{\delta \mathbf{e}_\alpha(\mathbf{x},t)} + \gamma_\alpha(\mathbf{x},t), \qquad \text{(S8)}$$

(Γ is the kinetic coefficient, $\gamma_\alpha(\mathbf{x},t)$ is the random Gaussian force, $\alpha = 1,2$), with the continuum limit of the Hamiltonian (1), cf. Ref. [S1, S2],

$$H = \frac{\rho_\perp}{2}\int d^2\mathbf{x}\left[(\nabla\mathbf{e}_1)^2 + (\nabla\mathbf{e}_2)^2 + V(\mathbf{e}_1,\mathbf{e}_2)\right], \qquad \text{(S9)}$$

where $\rho_\perp \approx \sqrt{3}J/4$ is the transverse spin stiffness. Since $\mathbf{S}_i^2 = 1$, Eq. (S7) implies $\mathbf{e}_1^2 = \mathbf{e}_2^2 = 1$, $\mathbf{e}_1\cdot\mathbf{e}_2 = 0$ at each lattice site $\mathbf{R}_i$, the potential $V(\mathbf{e}_1,\mathbf{e}_2)$ must have degenerate deep minima for these $\mathbf{e}_{1,2}$. Here we are interested only in the fluctuations of sufficiently low energies for which the potential V is reduced to a irrelevant constant which we choose to be zero.

Let there be an isolated vortex at the origin of coordinate system. If we neglect the spin-wave fluctuations (i.e. consider just a state with the lowest energy), the field configuration of the vortex,

$$\mathbf{e}_1 + \mathrm{i}\,\mathbf{e}_2 = e^{i\psi}\left(\mathbf{a} + \mathrm{i}\frac{\mathrm{x}\mathbf{b} + \mathrm{y}\mathbf{c}}{\sqrt{\mathrm{x}^2+\mathrm{y}^2}}\right), \qquad \text{(S10)}$$

is parametrized by three real orthonormal vectors $\mathbf{a}$, $\mathbf{b}$, $\mathbf{c}$ and angle ψ (x, y are the Cartesian coordinates in the plane of the lattice). Eq. (S10) shows that for general $\psi \neq \pi n/2$ (n is an integer) $\mathbb{Z}_2$-vortex is a non coplanar configuration. Nevertheless, the chirality vector

$$\mathbf{e}_3 = [\mathbf{e}_1\times\mathbf{e}_2] = \frac{-\mathrm{y}\mathbf{b} + \mathrm{x}\mathbf{c}}{\sqrt{\mathrm{x}^2+\mathrm{y}^2}} \qquad \text{(S11)}$$

describes an ordinary vortex which is planar in spin space. The energy of the configuration (S10)

$$H \approx \pi\rho_\perp \ln(R/a) \qquad \text{(S12)}$$

diverges logarithmically with the increase of the size of the system R (here a is the lattice spacing). Overall, if we neglect the spin-wave fluctuations, $\mathbb{Z}_2$-vortex is analogous to the vortex of the XY model (this analogy extends to the interaction between $\mathbb{Z}_2$-vortices which is also logarithmic).

However, the situation changes when one accounts for the spin waves, which wash out completely the vortex field configuration (S10) at distances $r \gg \xi_{\mathrm{sw}}$ from the center of the vortex owing to the finiteness of the correlation length ξ_{sw}. Here ξ_{sw} is equilibrium correlation length induced by spin waves without account for vortices.

Having performed a circuit around the vortex core at these distances and measuring $\mathbf{e}_{1,2}$ along the path, it will be impossible to determine from this information whether there is a vortex inside the contour or not. As a result, the energy of an isolated vortex E_1, renormalized by the spin-wave fluctuations, does not diverge with an increase of the system size; at temperatures $T \ll \rho_\perp$ this energy for an infinite system ($R = \infty$) behaves as [S3]

$$E_1 \approx \frac{3\pi^2\rho_\perp^2}{T} \propto \frac{T}{8}\ln(\xi_{\mathrm{sw}}/a)^2. \qquad \text{(S13)}$$

Similarly, the two vortices located at distances $r \gg \xi_{\mathrm{sw}}$ are almost do not interact with each other, and their energy $E_2 \approx 2E_1$. At shorter distances $r \lesssim \xi_{\mathrm{sw}}$ the double logarithmic attractive potential

$$U(a \ll r) = 2E_1 - E_2 \approx \frac{T}{4}\ln(\xi_{\mathrm{sw}}/r)^2 \qquad \text{(S14)}$$

emerges between vortices [S3].

Let us consider the relaxation of the high-temperature state within our coarse-grained description. Following Ref. [S4], we introduce the friction coefficient $\gamma(r)$ which

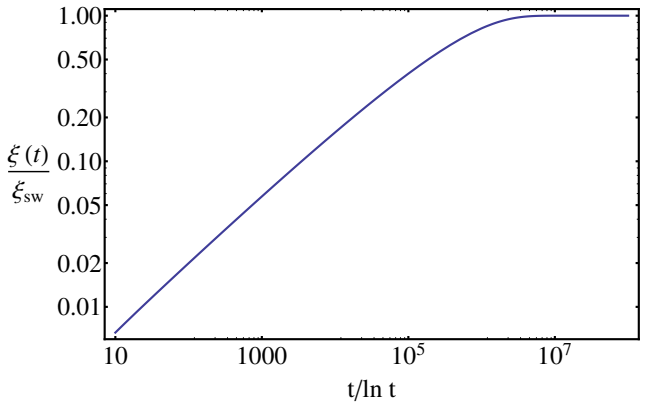

FIG. S4. Log-log plot of the function $\xi(t)$ satisfying equation (4), t is measured in units a^2/Γ.

depends on the distance between vortices. To calculate $\gamma(r)$ we consider the field configuration $\mathbf{e}_\alpha(\mathrm{x},\mathrm{y},t) = \mathbf{e}_\alpha(\mathrm{x}-vt,\mathrm{y},t)$ corresponding to two vortices augmented by arbitrary spin wave fluctuation and moving as a whole with the velocity v in direction x. Then the rate of energy dissipation is $dH/dt = \int d^2\mathbf{x}(\delta H/\delta\mathbf{e}_\alpha)\cdot(\partial\mathbf{e}_\alpha/\partial t) \approx -(1/\Gamma)\int d^2\mathbf{x}\sum_\alpha(\partial\mathbf{e}_\alpha/\partial t)^2 = -Hv^2/\Gamma$ (we have neglected the stochastic term in equation (S8), see Ref. [S4]). Hence, the friction coefficient equals $\gamma(r) = H/\Gamma$. Averaging over the spin-wave fluctuations we obtain

$$\gamma(r) = E_2/\Gamma \approx \frac{T}{4\Gamma}\left[\ln(\xi_{\mathrm{sw}}/a)^2 - \ln(\xi_{\mathrm{sw}}/r)^2\right]. \quad \text{(S15)}$$

Writing down the condition for the balance of the conservative $\mathbf{F} = -\nabla U(r)$ and the friction $-\gamma(r)d\mathbf{r}/dt$ forces we come to the equation

$$\frac{dr}{dt} = -f(r), \quad \text{(S16)}$$
$$f(r) = \frac{2\Gamma}{r}\frac{\ln(\xi_{\mathrm{sw}}/r)}{\ln(\xi_{\mathrm{sw}}/a)^2 - \ln(\xi_{\mathrm{sw}}/r)^2}, \quad a \ll r \lesssim \xi_{\mathrm{sw}}$$

(note that $f(r) > 0$ everywhere in the domain of applicability). According to this equation the fall of $\mathbb{Z}_2$-vortices at each other occurs in a finite time $\tau(r_0)$, which depends on initial distance between vortices r_0. The inverse function $\xi(t) = \tau^{-1}(t)$ satisfies the equation

$$\frac{d\xi}{dt} = f(\xi) \quad \text{(S17)}$$

and determines the time dependence of the dynamical correlation length $\xi(t)$. This equation is equivalent to the Eq. (4) of the main text. Even for $T \sim T_{BKT}$ the spin-wave correlation length ξ_{sw} has a very large value of order of several thousand lattice spacings, and typically $\xi(t) \ll \xi_{\mathrm{sw}}$ in the Monte Carlo calculations. In this regime $f(\xi) \approx \Gamma/(\xi\ln[\xi/a])$ has the same form as in the XY model [S4]. Accordingly, the solution of equation (4) gives the standard behavior of the correlation length $\xi(t) \propto (t\ln(t))^{-1/2}$. On the triangular lattice this regime exist up to rather long times $t \ll \xi_{\mathrm{sw}}^2/8\Gamma$. At even longer times, when $\xi(t)$ increases to the value of order ξ_{sw} the growth rate is slowing down. At $\xi = \xi_{sw}$ the equation (S16) gives $f(\xi) = 0$. Correspondingly, the dependence of $\xi(t)$ saturates (see Fig. S4). This should happen physically, because the equilibrium correlation length on a triangular lattice is finite at all nonzero temperatures. Thus, the result (S17) captures main features of the behavior of the dynamical correlation length which are expected physically and observed in the Monte Carlo simulation.

[S1] T. Dombre and N. Read, Phys. Rev. B **39**, 6797 (1989).
[S2] A. N. Ignatenko, V. Yu. Irkhin, and A. A. Katanin, Nucl. Phys. B **814**, 439 (2009).
[S3] A.N. Ignatenko. *To be published.*
[S4] A. J. Bray, A. J. Briant, and D. K. Jervis. Phys. Rev. Lett. **84**, 1503 (2000).